


The Intrinsic Blue Light Responses of Avian Müller Glial Cells Imply Calcium Release from Internal Stores

ASN Neuro
Volume 14: 1–13
© The Author(s) 2022
Article reuse guidelines:
sagepub.com/journals-permissions
DOI: 10.1177/17590914221076698
journals.sagepub.com/home/asn



Natalia A. Marchese^{1,2}, Maximiliano N. Ríos^{1,2} and Mario E. Guido^{1,2} 

Abstract

The retina of vertebrates is responsible for capturing light through visual (cones and rods) and non-visual photoreceptors (intrinsically photosensitive retinal ganglion cells and horizontal cells) triggering a number of essential activities associated to image- and non-image forming functions (photoc entrainment of daily rhythms, pupillary light reflexes, pineal melatonin inhibition, among others). Although the retina contains diverse types of neuronal based-photoreceptors cells, originally classified as ciliary- or rhabdomeric-like types, in recent years, it has been shown that the major glial cell type of the retina, the Müller glial cells (MC), express blue photopigments as Opn3 (encephalopsin) and Opn5 (neuropsin) and display light responses associated to intracellular Ca²⁺ mobilization. These findings strongly propose MC as novel retinal photodetectors (Rios et al., 2019). Herein, we further investigated the intrinsic light responses of primary cultures of MC from embryonic chicken retinas specially focused on Ca²⁺ mobilization by fluorescence imaging and the identity of the internal Ca²⁺ stores responsible for blue light responses. Results clearly demonstrated that light responses were specific to blue light of long time exposure, and that the main Ca²⁺ reservoir to trigger downstream responses came from intracellular stores localized in the endoplasmic reticulum. These observations bring more complexity to the intrinsic photosensitivity of retinal cells, particularly with regard to the detection of light in the blue range of visible spectra, and add novel functions to glial cells cooperating with other photoreceptors to detect and integrate ambient light in the retinal circuit and participate in cell to cell communication.

Summary statement:

Non-neuronal cells in the vertebrate retina, Müller glial cells, express non-canonical photopigments and sense blue light causing calcium release from intracellular stores strongly suggesting a novel intrinsic photosensitivity and new regulatory events mediating light-driven processes with yet unknown physiological implications.

Keywords

müller glial cells, Ca²⁺, blue light, endoplasmic reticulum, non-visual opsins, light sensitivity, retina

Received September 16, 2021; Revised December 28, 2021; Accepted for publication January 11, 2022

Introduction

The inner retina of vertebrates is a complex network of neurons and glial cells, nevertheless it shows a layered anatomic and functional arrangement, where the information flows both vertically and laterally (Guido et al., 2020; Meister & Tessier-Lavigne, 2013). Müller glial cells (MC) exhibit a key positioning across the whole retina, contacting all type of retinal neurons and together representing the smallest functional unit of the retina (Bringmann et al., 2006). Closely related to its location, numerous functions are attributed to MC spanning retinal development, metabolism, neurotransmission, injury response and regeneration (Barnett & Pow D, 2000; Bringmann et al., 2006; Jorstad et al., 2020; Newman, 2003; Pannicke et al., 2005; Pfeiffer-Guglielmi

¹CIQUIBIC-CONICET, Facultad de Ciencias Químicas, Universidad Nacional de Córdoba, Córdoba, Argentina

²Departamento de Química Biológica “Ranwel Caputto”, Facultad de Ciencias Químicas, Universidad Nacional de Córdoba, Córdoba, Argentina

Corresponding Authors:

Mario E. Guido, CIQUIBIC-CONICET, Facultad de Ciencias Químicas, Universidad Nacional de Córdoba, 5000 Córdoba, Argentina; Departamento de Química Biológica “Ranwel Caputto”, Facultad de Ciencias Químicas, Universidad Nacional de Córdoba, 5000 Córdoba, Argentina.
Email: mario.guido@unc.edu.ar

Natalia A. Marchese, CIQUIBIC-CONICET, Facultad de Ciencias Químicas, Universidad Nacional de Córdoba, 5000 Córdoba, Argentina; Departamento de Química Biológica “Ranwel Caputto”, Facultad de Ciencias Químicas, Universidad Nacional de Córdoba, 5000 Córdoba, Argentina.
Email: natalia.marchese@unc.edu.ar



et al., 2005; Willbold et al., 2000). Notably, MC have engaged diverse research field for many years as for comparative, morphological and basic neuron-glia interaction studies of great significance (Newman, 2005, 2015; Pannicke et al., 2017).

Local circuits in the inner retina of vertebrates drive specific non-image forming functions (NIF) that include, among others, the entrainment of circadian rhythms at cellular, molecular and metabolic levels. The information regarding environmental lighting conditions along the day in the blue-UV spectrum is processed by non-canonical photoreceptor cells and non-visual opsins (Opn3/encephalopsin, Opn4/melanopsin and Opn5/neuroopsin) (Berson et al., 2002; Buhr et al., 2015; Chaurasia et al., 2005; Contin et al., 2006; Hattar et al., 2003; Lucas et al., 2003; Morera et al., 2016; Rios et al., 2019). Our group has substantially contributed to the identification of new retinal photosensitive components by initially describing the pupillary reflex action spectrum in the blind chick strain named GUCY1* - which has complete loss of rods and cones from the time of hatching- with an absorbance peak at 484 nm (Valdez et al., 2009). Strikingly, these blind birds suffering a severe retinal degeneration retain their inner retina functional and still able to synchronize their feeding rhythms to light (Valdez et al., 2009, 2013). In particular, a subpopulation of intrinsically photosensitive retinal ganglion cells in the chicken retina activates the phosphoinositide cycle as well as an increase in intracellular Ca²⁺ levels (Contin et al., 2006; Contin et al., 2010; Díaz et al., 2017). Moreover, horizontal cells expressing Opn4x (Xenopus isoform) were later characterized as new intrinsic photoreceptors responding to light through a cascade involving Gq protein, phospholipase C (PLC) activation, depolarization and increased intracellular Ca²⁺, with consequent release of the inhibitory neurotransmitter GABA (Morera et al., 2016). In both cases the photosensitive capacity of these cells was attributed to the expression of the non-visual photopigment Opn4 (Díaz et al., 2017; Morera et al., 2016). Meanwhile, activation of Opn4x in chicken retinal ganglion cells and the photoisomerase retinal G protein-coupled receptor (RGR) in MC modulate retinaldehyde levels in response to light and maintain the balance of inner retinoid stores (Díaz et al., 2017).

Our most recent studies are focused on light-driven responses in MC, at first by the description of a gradual increase, from early embryonic stages (E7/8) throughout development and up to the time of hatching, in the transcription and expression of Opn3. The staggering increase of the non-visual opsin expression goes along with the elevation in transcription and expression of classical glial markers, such as glial fibrillary acidic protein (GFAP) and glutamine synthase (GS) (Rios et al., 2019). In fact, MC in primary cultures express the non-visual opsins Opn3 and Opn5, and particularly for Opn3 we showed that its expression and location is photic-regulated by blue light (BL) and dependent on protein synthesis. Further, we identified a direct photic response by

MC to a BL pulse observed as an increase in intracellular Ca²⁺ levels. This response is dependent on opsin activation, as it is inhibited by the non-specific opsin antagonist hydroxylamine, and identifies three subpopulations based on their BL responses: cells responding with $\geq 20\%$ of Ca²⁺ increase, another group with 10–20% of Ca²⁺ increase, and those not responding at all (Rios et al., 2019).

The present work describes to a greater extent the Ca²⁺ response elicited by a BL pulse in enriched cultures of avian MC. We show that MC activation involves Ca²⁺ release from intracellular stores; as their pharmacological depletion decreased the percentage of MC effectively responding to BL whereas the presence of an extracellular Ca²⁺ chelator did not substantially affect BL responses. Indeed, cytosolic Ca²⁺ increase in MC goes along with a decrease in the levels of Ca²⁺ in the endoplasmic reticulum. In this context, MC can be postulated as new intrinsically photosensitive components in the inner retina of vertebrates potentially contributing to local circuits in the regulation of various physiological processes by BL.

Materials and Methods

Materials

All reagents were of analytical grade. Opn3 Polyclonal Antibody, Rabbit (NovusCat# NB110-74721, RRID:AB_2158340); Vimentin monoclonal antibody, Mouse (Sigma-Aldrich Cat# V5255, RRID:AB_477625); GFAP polyclonal antibody, Rabbit (Sigma-Aldrich Cat# G9269, RRID:AB_477035); Glutamine Synthetase monoclonal antibody, Mouse (Millipore Cat# MAB302, RRID:AB_2110656); Glutamate/Aspartate transporter 1 (Santa Cruz Cat#sc-515839); and Tubulin monoclonal antibody, Mouse (Sigma-Aldrich Cat# T9026, RRID:AB_477593). The secondary antibodies used for immunocytochemistry were DylightTM 488-conjugated AffiniPure Donkey Anti-Mouse or DylightTM 549-conjugated AffiniPure Donkey Anti-Rabbit (dilution 1:1,000, Jackson Immuno Research Laboratories). 40,6-diamidino-2-phenylindole (DAPI), papain suspension in 0.05 M sodium acetate (P3125), trypsin, Thapsigargin and EGTA were from Sigma-Aldrich. The fluorescent Ca²⁺ indicators Calcium Orange/AM, Mag-Fluo-4/AM or Rhod-2/AM were from Invitrogen-Molecular Probes

Animal Handling

For the different studies performed, chicken embryos (*Gallus gallus domesticus*) (Avico) at embryonic day 8 (E8) were used as previously described (Díaz et al., 2017; Rios et al., 2019). Eggs were incubated at 37°C with 60% of humid atmosphere (model 80/AD, Yonar SRL, Buenos Aires, Argentina). Chicken embryos were sacrificed by decapitation. All experiments were performed in accordance with the Use of Animals in Ophthalmic and Vision Research of ARVO, approved by

CICUAL (Institutional Committee for the Care and Use of Experimental Animals, School of Chemistry, National University of Cordoba; RD-2021-717-E-UNC-DEC#FCQ).

Primary Cultures of Müller Glial Cells

Primary cultures of MC were purified from neural chick E8 retinas. Briefly, retinas were dissected in ice-cold Ca^{+2} - Mg^{+2} free Tyrode's buffer (CMF) containing 25 mM glucose as previously reported (Díaz et al., 2017) with modifications (Rios et al., 2019). Briefly, cells were treated with papain for 25 min at 37°C and trypsin for 5 min and rinsed with Fetal Bovine Serum (FBS) 10% and Dulbecco's modified Eagle's medium (DMEM- Sigma). After dissociation, the cells in suspension were seeded in Petri dishes and were grown in DMEM supplemented with FBS 10% for two weeks. After 7 days, cell cultures are trypsinized and re-plated in petri dishes or multiwell depending on the experiment and maintained for another week, when we obtain purified glial cultures, virtually free of neurons. Cultures were incubated at 37°C under constant 5% CO_2 -air flow in a humid atmosphere (MCO 175, SANYO). Primary cell cultures were characterized according to different glial cell markers such as GFAP, glutamine synthetase (GS), and Glutamate-aspartate Transporter (GLAST1, EAAT1) under basal conditions to determine the glial identity of cells present in the cultures (Suppl. Fig. 1). Results showed that most cells in the cultures co-express GFAP together with GS or GLAST1, strongly indicating that they are retinal MC.

Immunocytochemistry (ICC)

Cultured cells were fixed for 15 min in 4% paraformaldehyde in phosphate-buffered saline (PBS) and washed in PBS, treated with blocking buffer (3% bovine serum albumin, 0.1% Tween 20, 1% glycine, 0.02% sodium azide in PBS) and incubated overnight with the primary antibodies fo: Opn3 (1:500); Vimentin (1: 1,000); Glutamine Synthetase (1: 1,000); GLAST (1:500); GFAP (1: 1,000). They were then rinsed in PBS and incubated with the secondary antibodies (1: 1,000) for 1 h at RT. Samples were incubated with DAPI (3 μM). Coverslips were finally washed thoroughly and visualized by confocal microscopy (FV1200; Olympus, Tokyo, Japan) (Morera et al., 2012; Rios et al., 2019).

Calcium Imaging by Fluorescence Microscopy

Cells were grown in an 8-well Lab-Tek recording chamber (Nunc™, NY-USA). On the day of the experiment, MCs were incubated with 0.1% of pluronic acid F-127 and 5 μM of the Ca^{2+} indicator dye, in a colorless DMEM for 1 h at 37°C, under darkness condition. The cells were washed three times with CMF and then Ca^{2+} was measured in DMEM by exciting the indicator at 488 nm (Mag-Fluo-4/AM) or 543 nm (Calcium Orange/AM and Rhod-2/AM) for

1 min. Cells were then stimulated with a BL pulse (20 s; 470–490 nm, peak at 480 nm LED of 85 $\mu\text{W}/\text{cm}^2$), a red-light pulse (20 s; 630–650 nm, peak at 640 nm LED of 48 $\mu\text{W}/\text{cm}^2$) or Ionomycin, 2 μM for positive control as previously described (Rios et al., 2019), and imaged for another 5–8 min. In order to identify the source of Ca^{2+} in light-driven response in MC, Thapsigargin (TG 2 μM) and EGTA (100 μM) were added to the medium for at least 20 min before commencing the recordings. The fluorescence imaging technique was performed by confocal microscopy with an Olympus FluoView- 1,000 microscope. The emitted fluorescence was captured every 2 s, using a PlanApo N 60 \times Uplan SApo oil-immersion objective (NA: 1.42; Olympus).

Image Processing

The 12 bit 4×4 binned fluorescence images for each photo were used to quantify fluorescence levels in the cells using ImageJ software. The Ca^{2+} fluorescence intensity ratio (F/F_0) was plotted as a function of time in figures. Approximately 150 cells were analyzed from at least two independent experiments; the mean from all experiment is plotted in Figures 2, 4 and 5. At each time point, changes in fluorescence levels in selected regions of interest were quantified as the ratio between the relative intensity level measured after a BL pulse and the mean of intensities of serial pictures before stimulation (F_0) (Morera et al., 2016; Rios et al., 2019). Fluorescence intensities during light stimulation were not considered for the analyzes and are shown as arbitrary values of $F/F_0 = 1$. Moreover, total average changes in fluorescence intensities along the whole experiment after the stimulus are expressed as ΔF and compared between experimental groups or against a theoretical mean of no change ($\Delta F = 1$) when indicated. Values of F/F_0 are not linearly related to changes in $[\text{Ca}^{2+}]_i$ but are intended to provide a qualitative indication of variations in $[\text{Ca}^{2+}]_i$. No significant vehicle effects or changes in focus were detected. Responses were considered significant when the ratio at the peak differed from the baseline levels by at least 10%.

Prolonged Light Treatment

To test possible deleterious effect of BL stimulus over primary cultures of MC prolonged light exposure was conducted by pre-incubating MC for 1 h in DMEM, then cell cultures were then divided into three groups: darkness control (dark), BL stimulation for 1 h (BL, 480 nm) for 1 h (BL 1 h, LED of 85 $\mu\text{W}/\text{cm}^2$), and darkness condition for 1 h after the BL stimulation (1 h post).

RNA Isolation and Polymerase Chain Reaction

Total RNA from MC cultures was extracted using the TRIzol™ kit for RNA isolation (Invitrogen). RNA integrity was checked and quantified by UV spectrophotometry (Epoch

Microplate Spectrophotometer, Biotek). Finally, 2 mg of total RNA was treated with DNase (Promega) to eliminate contaminating genomic DNA. cDNA was synthesized with M-MLV (Promega) using Random Primers (Promega) as previously described in Rios et al. (2019). The oligonucleotide sequences used for PCR from the *G. gallus* sequences were as follows:

Opn3:

Forward GCCTCTTCGGGATCGTTTCA
Reverse ATGTGATAGCCCGCCAAGAC

TATA-binding protein (TBP):

Forward TGGCACACGAGTAACAAGAG
Reverse CCTTGAGCGTCAGGGAAATAG

For Polymerase Chain Reaction initial denaturation step was set for 1 min at 94°C, 35 cycles of 60 s at 94°C, 50 s at 60–65°C, 90 s at 72°C, and a final 5 min elongation step at 72°C. Amplification products were separated by 2% agarose gel electrophoresis and visualized by ethidium bromide or SyberSafe (Invitrogen™) staining.

Western Blot

Homogenates of primary MC cultures were resuspended in RIPA buffer [50 mM Tris-HCl, pH 8.0, with 150 mM sodium chloride, 1.0% Igepal (NP-40), 0.5% sodium deoxycholate, and 0.1% sodium dodecylsulfate] containing protease inhibitors (Sigma-Aldrich) and processed for western blot (WB) according to Rios et al. (2019). Homogenates were resuspended in sample buffer and separated by SDS-gel electrophoresis on 12% polyacrylamide gels (50 mg total protein/lane), transferred onto Polyvinylidene fluoride (PVDF) membranes, blocked for 1 h at RT with 5% BSA in PBS, and then incubated overnight at 4°C with specific antibodies against GFAP (1: 1,000) and tubulin (1: 2,000) in the incubation buffer (3% BSA, 0.1% Tween 20, 1% glycine, 0.02% sodium azide in PBS). Membranes were washed three times for 15 min each in washing buffer (0.1% Tween 20 in PBS) and incubated with the corresponding secondary antibody in the incubation buffer during 1 h at RT followed by three washes with washing buffer for 15 min each. Membranes were scanned using an Odyssey IR Imager (LI-COR Biosciences).

Cell Viability by MTT Assay

MC enriched cultures were replicated in 96-well plates and grown for 4 days at 37°C. Cells were divided into three groups: dark (control), BL for 1 h and sodium arsenite (ARS, 500 µM for 1 h as positive control). After treatment, the medium was removed and replaced by 10% FBS in DMEM and cells were kept in darkness for 24 h at 37°C. Then, as described by Wagner et al. (2019) and Rios et al. (2019), MTT reagent (5 mg/mL; Sigma) was added to each well, plates were further incubated for 2 h at 37°C; followed by addition of 100 µL of DMSO:isopropanol (1:1, v/v) and

incubation for a few minutes at room temperature, protected from light. Samples were analyzed at a wavelength of 570 nm with a reference at 650 nm in an Epoch Microplate Spectrophotometer. Cell viability was analyzed by considering average value in darkness conditions as 100% of viability

Cell Viability by Flow Cytometry

Cell viability was analyzed in MC cultures maintained in the dark and incubated with EGTA (100 µM) or TG (2 µM) for 1 h. Then, the culture medium was removed and cells were washed with PBS 1X and harvested by trypsinization. After centrifugation at 3,000 rpm for 3 min, trypsin was removed and cells were incubated in 200 µL of PBS 1X with Calcein Red-Orange 3 µM (Invitrogen) and DAPI (Sigma) at 2 µM final concentration for 15 min at room temperature. The fluorescence intensity was measured by flow cytometry, using BD LSRFortessa, at 583 nm when the sample was excited at 485 nm for Calcein dye (to identify live-cells population) and 421/405 nm for DAPI (for dead-cells population). Cells without the fluorescent indicators were used as negative control. FlowJo software was used to analyze the live and death population. Cytotoxic effects of drug treatment alone over MC cultures were discarded after assessing cell viability after 1 h of incubation with EGTA or TG (Suppl. Figure 3).

Statistics

Statistical analyzes involved a t-test or one-way analysis of variance (ANOVA) followed by Bonferroni post-hoc comparison when appropriate. Otherwise, Mann-Whitney (M-W) or Kruskal-Wallis (K-W) tests were used when normal distribution or homogeneity of residuals was infringed with pairwise comparisons performed by the Dunn's test when appropriate. Analyzes for frequency distribution and Gaussian model were performed by non-linear fit regression. In all cases significance was considered at $p < 0.05$.

Results

We further characterized BL responses in MC expressing the BL-sensitive opsin Opn3 by looking at the main sources of Ca²⁺ in these cells and differentially affecting intracellular and extracellular Ca²⁺ availability; further describing the intracellular Ca²⁺ mobilization by specific compartment Ca²⁺ indicators.

Müller Glial Cells Expressing Opn3 Display Calcium Increase Specifically Triggered by a Blue Light Pulse

Primary cultures of avian retina prepared at E8 and maintained for 2 weeks were highly enriched in MC exhibiting the typical glial morphology and showing positive

immunoreactivity for the glial markers Vimentin (Figure 1A), GS, GFAP and GLAST1 (Suppl. Fig. 1) whereas the expression of the non-visual opsin Opn3 was also detected at the levels of mRNA and protein (Figure 1A, Suppl. Figure1).

A well-known feature of cells displaying intrinsic photosensitivity is related to significant changes in intracellular Ca^{2+} levels (Contín et al., 2010; Díaz et al., 2017; Morera et al., 2016; Nieto et al., 2011; Rios et al., 2019). Thus, we initially assessed changes in intracellular Ca^{2+} levels by fluorescent imaging with Calcium orange in cell cultures after photic stimulation with blue/red wavelengths (Figure 1B and C). In this sense, we identified a direct and specific photic response to a BL pulse ($85 \mu\text{Watt}/\text{cm}^2$ for 20 s) observed as an increase in relative intracellular Ca^{2+} levels in individual MC (mean values across time up to more than 20%, and significantly different to a theoretical mean = 1; $p < 0.01$ by t test); whereas red light stimulation ($48 \mu\text{Watt}$, 20 s) did not evoke significant Ca^{2+} responses (N.S., $p > 0.05$ by t test); in fact, the overall Ca^{2+} levels in MC after BL stimulation differed from those after a red light pulse ($p < 0.001$ by t test) (Figure 1B and C).

Gliosis was evaluated under different conditions to discard any possibility of bias in the results due to the characteristic glial response under pathological conditions. First we determined whether MC in culture differentially expressed GFAP (Suppl. Fig. 1). Under basal conditions, most cells in the culture expressed detectable, normally distributed levels of GFAP, therefore indicating that different subpopulations of GFAP-expressing MC are implausible. Moreover, these GFAP (+) cells co-localized with GS and GLAST1. Moreover no differences were observed in GFAP levels after 1 h of continuous BL stimulation ($85 \mu\text{Watt}/\text{cm}^2$), or 1 h in darkness after the BL stimulus (1 h post BL) as compared with basal controls in the dark; nor were there any differences in the level of cell viability, with no significant differences between dark and prolonged BL stimulation (Suppl. Figure 2). Taken together these results strongly indicate that neither gliosis nor any other deleterious effect occurred under the experimental conditions tested. In addition, no significant deleterious effect of BL stimulation has been observed in primary cultures of retinal neurons (Rios et al., unpublished data), which is consistent with results

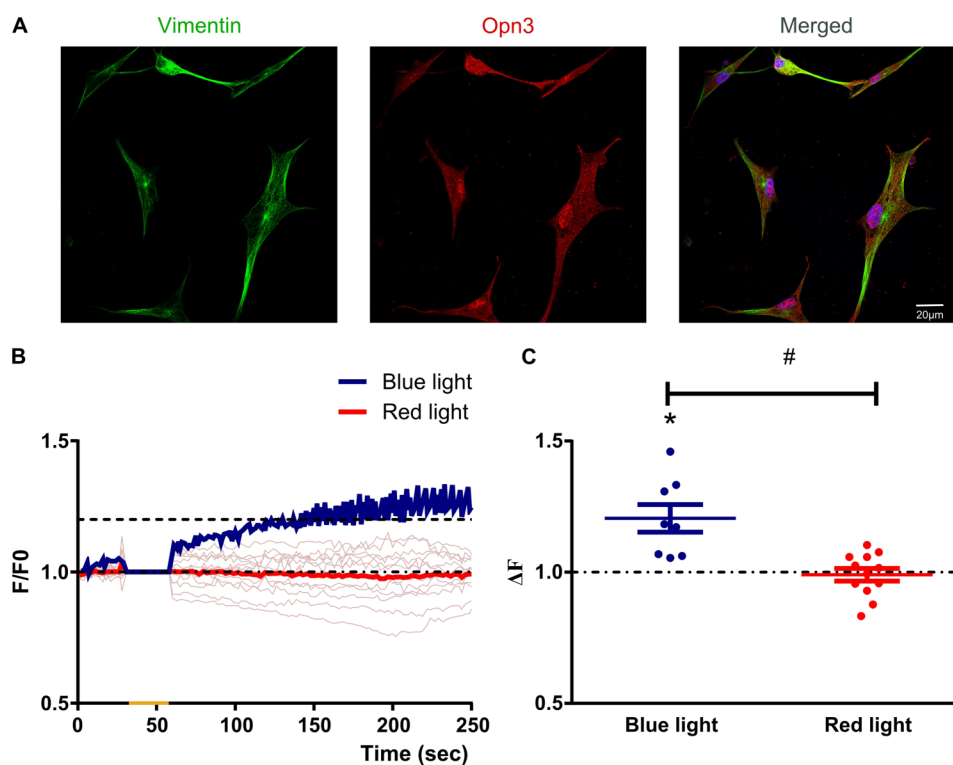


Figure 1. Müller glial cells express blue light-sensitive opsins and display calcium increase specifically in response to blue light stimulation. (A) Primary cultures highly enriched in Müller glial cells as defined by morphological cell identification (non-neuron like morphology) and the glial marker Vimentin expression (green) were labeled for Opn3 (red) and visualized by confocal microscopy. Müller cells showed ubiquitous and generalized localization of Opn3. Scale bar = 20 μm . (B) Graphical representation showing the mean F/F₀ ratio for Ca^{2+} responses in Müller cells when exposed to a single brief light pulse for 20 s (yellow mark) within the blue or red wavelengths (Blue and red lines respectively- light red lines show individual recording with red light stimulus). (C) Graphical representation of relative fluorescent Ca^{2+} levels (ΔF) in Müller cells when exposed to a single brief blue or red light pulse. The graph shows individual values with the media \pm SEM. A t test revealed a significant effect in overall Ca^{2+} levels with blue light stimulation as compared to a theoretical mean of no change ($\Delta F = 1$; $t_{(7)} = 3.90$, $**p < 0.01$) and red light stimulation ($t_{(18)} = 4.16$, $\#p < 0.001$) (20 cells from 2 independent experiments).

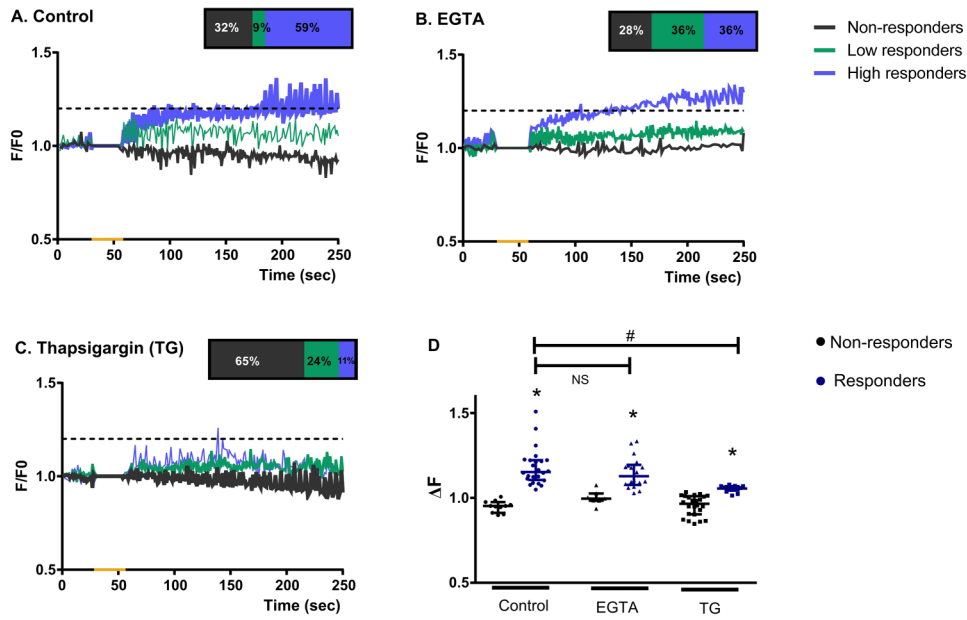


Figure 2. Internal stores are the main source for calcium increase in Müller glial cells in response to blue light stimulation. Graphical representation showing the mean F/F₀ ratio for Ca²⁺ responses in Müller cells when exposed to a blue light pulse (20 s- yellow mark) under control conditions (A), in presence of the extracellular Ca²⁺ chelator EGTA (100 μM) (B), and treated with the SERCA inhibitor TG (2 μM) (C). In all cases, the graphs show the mean values of the F/F₀ ratio for three different Ca²⁺ responses: High responders (blue lines); low responders (green lines) and non-responders (gray lines). Lines thicknesses are representative of cell percentage for each type of response in the different conditions tested. The insets in the three experimental conditions (A), (B) and (C) show the percentage of the different Ca²⁺ responses in Müller glial cells after a blue light pulse: high- (blue); low- (green) and non-responders (gray). (D) Graphical representation of the overall relative fluorescent Ca²⁺ levels (ΔF) elicited by a blue light pulse in Müller glial cells under the different experimental conditions (control, EGTA 100 μM and TG 2 μM). For each treatment, the graph shows individual values with the median with range for non-responders (black) and responders cells (High and Low responders- Blue). A Kruskal Wallis test revealed significant different Ca²⁺ levels ($H_{(5)} = 76.74$; $p < 0.0001$) and the Dunn's multiple comparison indicated that for each experimental condition cells responding with an increase in Ca²⁺ levels show significant higher values as compared with non-responders in the same condition (* $p < 0.05$; ** $p < 0.01$; *** $p < 0.0001$). Dunn's test also indicates that the overall Ca²⁺ levels in TG increase group are lower than those observed with light stimulation under control conditions (# $p < 0.05$) (96 cells from 3/4 independent experiments).

obtained by other groups using similar photic conditions (Mansoor et al., 2015).

Internal Stores are the Main Source for Calcium Increase in Müller Glial Cells by Blue Light Stimulation

In order to identify the main source of Ca²⁺ in MC light-driven activation, we evaluated Ca²⁺ responses elicited by a BL pulse (68 μW/cm² for 20 s) in the presence of an extracellular Ca²⁺ chelator (EGTA 100 μM, 30 min) or after depletion of Ca²⁺ internal stores with TG (2 μM, 40 min) (Figure 2 and 3).

In line with our previous results (Rios et al., 2019), we identified a not responding subpopulation of MC to BL with no Ca²⁺ increase (32%; Figure 2A, gray lines -non-responders-); whereas 68% of the registered MC actually did respond to the BL stimulus with an increase in intracellular Ca²⁺ levels according to the following distribution: 9% of cells showed a 10–20% increase in Ca²⁺ fluorescence

levels over the basal threshold (Figure 2A, green lines -low responders-), while another subpopulation of cells (59%) responded with a higher than 20% increase in Ca²⁺ levels (Figure 2A, blue lines -high responders-). Similar results were obtained in presence of EGTA where 72% of MC responded to BL stimulation while 28% did not exhibit detectable responses (Figure 2B). Under this condition, the percentage of cells responding over the basal threshold (low and high responders) was ~36% in both cases (Figure 2B). Interestingly, pre-incubation with TG increased the percentage of non-responders MC up to 65% (Figure 2C) and the remaining percentage of cells showed low Ca²⁺ responses (24%) and only 11% of MC reached more than 20% increase over the basal threshold (high responders, Figure 2C). For all experimental groups, relative fluorescent Ca²⁺ levels (ΔF) analysis indicated a significant increase in the MC responding subpopulation (shown as responders in the graph and including high and low responders) as compared with fluorescence values in non-responder MC ($p < 0.0001$ by Kruskal-Wallis test) (Figure 2D).

Since there is a MC subpopulation that does not respond to BL stimulation in basal conditions (control group) (Figure 2A, (Rios et al., 2019)), further analyzes were performed excluding this percentage of cells in each experimental group (Figure 3A). In this case, under control conditions 87% of the cells effectively responding to BL stimulation are high responders. This percentage was modified to 50% by EGTA treatment (Figure 3A); however the remaining 50% still showed low Ca²⁺ responses (Figure 3A) and the overall Ca²⁺ responses (ΔF for responders) did not differ from those in control groups (non-responders; N.S., $p > 0.05$ by Dunns' multiple comparison test) (Figure 2D). For the TG conditions we observed that among MC that are expected to respond, only 15% of them were high responders to BL stimulation (Figure 5A); otherwise, TG effectively suppressed Ca²⁺ responses in 50% of this MC subpopulation (Figure 3A) and significantly decreased the overall Ca²⁺ response (ΔF in responders groups) of MC that still showed Ca²⁺ increased levels when compared to control groups (non-responders; $p < 0.05$ by Kruskal-Wallis test) (Figure 2D).

TG is a well-established pharmacological tool that modifies Ca²⁺ availability from internal stores in a time dependent manner (Carpio et al., 2021; Morera et al., 2016). Short periods of time promote Ca²⁺ release from the endoplasmic reticulum to the cytosol as well as Ca²⁺ transfer from the endoplasmic reticulum to the mitochondria (Carpio et al., 2021); meanwhile long time periods effectively deplete Ca²⁺ internal stores (Morera et al., 2016). These conditions were evaluated and corroborated in our present model (Suppl. Fig. 4) as 20 min TG incubation did not affect the BL response of MC compared to control and a theoretical mean of $\Delta F = 1$ ($p < 0.05$ by Wilcoxon and Kruskal-Wallis test, Suppl. Fig. 4B); whereas incubation for 40 min effectively suppressed Ca²⁺ responses to BL ($p > 0.05$ by Wilcoxon and Dunns' multiple comparison test, Suppl. Fig. 4B). In addition, the Ca²⁺ ionophore ionomycin (2 μM) was used as a positive control as previously described (Rios et al., 2019). Even though Ca²⁺ availability is modified in both conditions (EGTA and TG treatments), an increase

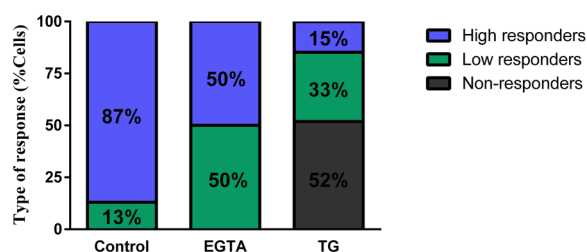


Figure 3. Calcium increase in müller glial cells by blue light is affected by depletion of internal stores. Graphical representation for the percentage of Ca²⁺ responses within Müller glial cells that effectively respond or are expected to respond to a blue-light pulse. The Ca²⁺ increase triggered by the brief BL pulse is suppressed in 50% of Müller glial cells with TG incubation, suggesting an internal store-operated Ca²⁺ response.

in Ca²⁺ levels promoted by ionomycin was still detectable in MC by the Ca²⁺ indicator dye Calcium Orange AM ($p < 0.05$ and $p < 0.01$, respectively, compared to theoretical mean = 1 by Wilcoxon test, Suppl. Fig. 5). Taken together, results obtained demonstrate that intracellular stores constitute the main Ca²⁺ reservoir to trigger significant BL responses in MC assessed by Ca²⁺ mobilization.

Calcium is Released from the Endoplasmic Reticulum in Response to Blue Light Stimulation in Müller Glial Cells

Methods that employ chemical indicators with a fluorescent response upon Ca²⁺ binding are particularly powerful and can be used to differentially study Ca²⁺ from diverse and particular sources (Carpio et al., 2021; Carpio & Katz, 2019). Bearing this in mind, we next focused on BL-driven Ca²⁺ responses in different cellular compartments of MC, by combining cytosolic and endoplasmic reticulum Ca²⁺ dyes (Calcium Orange/AM and Mag-Fluo-4/AM respectively); whereas mitochondrial Ca²⁺ levels were analyzed with Rhod-2/AM in a different subset of MC (Figure 4A). Once again we identified three subpopulations of MC with similar percentages as described in previous section: non-responders (29%, Figure 4B, gray lines); low responders (24%, Figure 4B, green lines); and high responders (47%, Figure 4B, blue lines). On the other hand, when Ca²⁺ signals from the endoplasmic reticulum were analyzed we identified that 50% of MC did not show any Ca²⁺ increase (Figure 4C), whereas the remaining population did so by increasing Ca²⁺ levels between 10–20% (18%, Figure 4C) or more than 20% (32%, Figure 4C) over the basal threshold. For both Ca²⁺ indicators the overall Ca²⁺ response (ΔF) in MC responding to the blue light pulse (high and low responders) was significantly different from those not responding with Ca²⁺ variations ($p < 0.0001$ by Kruskal-Wallis test, Figure 4E). Regarding mitochondrial Ca²⁺ levels, 67% of analyzed MC did not show any increase in Ca²⁺ content while the 33% left reached low Ca²⁺ responses (Figure 4D); however the overall Ca²⁺ response (ΔF) in mitochondria did not differ among responders and non-responders groups (N.S. $p > 0.05$ Dunns' multiple comparison test, Figure 4E).

Taking advantage of the combined use of Ca²⁺ indicator dyes we evaluated Ca²⁺ signals from cytoplasm and endoplasmic reticulum by considering two groups: MC responding with cytosolic Ca²⁺ increase and MC with no increase in cytosolic Ca²⁺ after BL stimulation (cytosolic increase and no increase groups respectively, Figure 5 and 6). Interestingly, the time line for the cytosolic Ca²⁺ increase in MC fitted with a decrease over time in Ca²⁺ levels in the endoplasmic reticulum (Figure 5A). Indeed, the relative fluorescent Ca²⁺ levels (ΔF) analysis indicated significant higher and lower values for cytosolic ($p < 0.0001$ by t test;

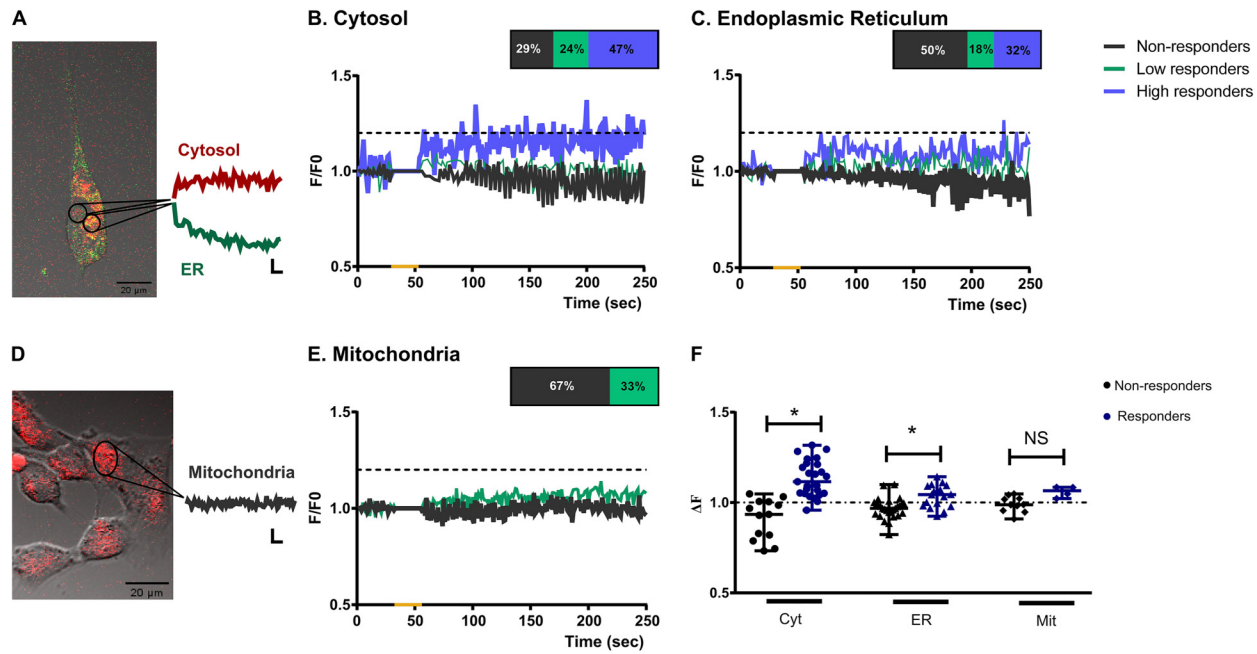


Figure 4. Calcium responses to blue light in Müller glial cells differ among cellular compartments. Representative Müller cells kept in culture for two weeks loaded with Calcium Orange/AM and Mag-Fluo-4/A (**A**), or Rhod-2/AM (**D**). Scale bar = 20 μ m. The right panels show the individual trace for each ROI record with the different Ca²⁺ indicators after a blue light pulse (BL) of 20 s. Scale bars: vertical = 20% increase; horizontal = 20 s. Graphical representation showing the mean F/F₀ ratio for Ca²⁺ responses in Müller cells when exposed to a blue light pulse (20 s - yellow mark) for the different Ca²⁺ indicators: Calcium Orange/AM for cytosolic Ca²⁺ (**B**), Mag-Fluo-4/A for measuring Ca²⁺ in endoplasmic reticulum (**C**), and Rhod-2/AM for mitochondrial Ca²⁺ levels (**E**). In all cases, the graphs show the mean values of the F/F₀ ratio for three different Ca²⁺ responses: High responders (blue lines); low responders (green lines) and non-responders (gray lines). Lines thicknesses are representative of cell percentage for each type of response with the different dyes. The insets in **B**, **C** and **E** show the percentage of the different Ca²⁺ responses in Müller glial cells after a blue light pulse: high- (blue); low- (green) and non-responders (gray). (**F**) Graphical representation of the overall relative fluorescent Ca²⁺ levels (ΔF) elicited by a blue light pulse in Müller glial cells; within each compartment (Cytoplasm, endoplasmic reticulum and mitochondria) values are shown for non-responder (Black) and responder MC (High and Low responders - Blue). The graph shows individual values with the median with range. A Kruskal Wallis test revealed significant different Ca²⁺ levels ($H_{(5)} = 48.90$; $p < 0.0001$) and the Dunn's multiple comparison indicated that cells responding with an increase in Ca²⁺ levels show significant higher values as compared with non-responders for cytosolic and endoplasmic reticulum Ca²⁺ indicator dyes ($*p < 0.05$; $***p < 0.0001$).

$t_{(24)} = 6.67$) and endoplasmic Ca²⁺ ($p < 0.01$ by t test, $t_{(24)} = 2.84$) respectively, as compared with a theoretical mean of no change = 1 (Figure 6). On the contrary, MC with no cytosolic Ca²⁺ increase showed correspondence with the endoplasmic Ca²⁺ recordings indicating increased levels along time (Figure 5B). In this case, the overall Ca²⁺ levels (ΔF) were significantly lower for cytosolic ($p < 0.05$ by t test, $t_{(12)} = 2.92$) and higher for endoplasmic Ca²⁺ levels ($p < 0.05$ by t test, $t_{(12)} = 2.78$) respectively as compared with a theoretical mean of no change = 1. Mitochondrial Ca²⁺ levels are shown as control group with no significant changes in Ca²⁺ fluorescence levels ($p > 0.05$ by t test, $t_{(13)} = 0.72$) (Figure 6). As a positive control, a series of experiments were performed in the presence of 2 μ M ionomycin (Suppl. Fig. 6A), known to promote the intracellular mobilization of Ca²⁺, in which significant increases in Ca²⁺ fluorescence were detected for all Ca²⁺ dyes tested as compared with a theoretical mean of no change = 1 ($p < 0.001$ by t test, Suppl. Fig. 6B).

Discussion

In order to drive NIF activities, the inner retina of vertebrates has developed along the evolution the capacity to detect the quality of light irradiance across the day. Bearing in mind that the amount, spectral composition and source of light changes systematically as the day goes by, it is not surprising the great diversity of non-visual opsins described up to date (Guido et al., 2020; Peirson et al., 2009). The photoreception capacity of these pigments is mainly concentrated in the blue region of the spectrum (around 480 nm, with higher energy), which represents a conserved feature across species possibly related to the penetrance of this particular wavelength and to the spectral composition of light at twilight (Davies et al., 2010; Guido et al., 2020; Peirson et al., 2009). MC have been identified among the cells expressing these non-visual photopigments and, particularly in the avian retina, MC have been shown to express Opn3, Opn5 and RGR (Figure 1A, (Díaz et al., 2017; Rios et al., 2019)). Our

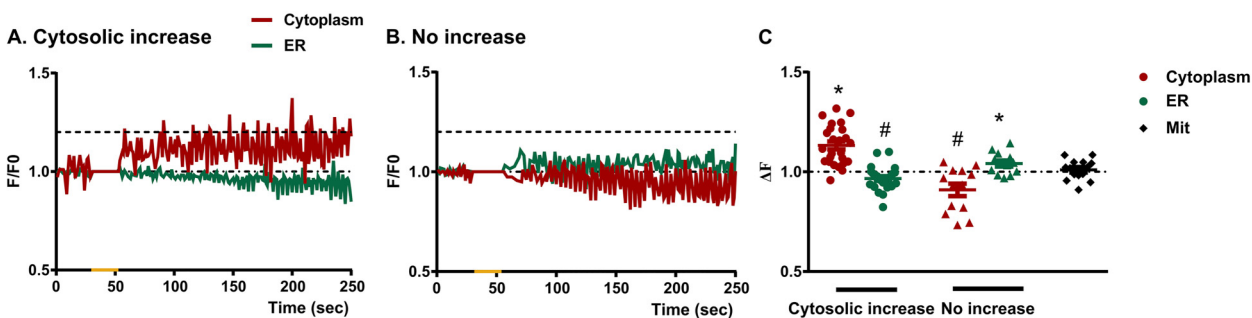


Figure 5. Blue light-triggered cytosolic calcium increase in Müller glial cells mirrors the calcium decrease in endoplasmic reticulum. Graphical representation showing the mean F/F_0 ratio considering the two main type of cytosolic Ca^{2+} responses in Müller cells: Ca^{2+} increase (A) / No Ca^{2+} increase (B), when exposed to a blue light pulse (20 s- yellow mark). The graphs show the mean values of the F/F_0 ratio for three different Ca^{2+} responses: Ca^{2+} + Orange/AM (red lines- cytosolic Ca^{2+} +) and Mag-Fluo-4/A (green lines, endoplasmic Ca^{2+} +) (C) Graphical representation of the overall relative fluorescent Ca^{2+} levels (ΔF) elicited by a blue light pulse in Müller glial cells; for each type of cytosolic Ca^{2+} response (Cytosolic increase/No increase) values are shown for cytosolic and endoplasmic reticulum indicator dyes (red and green, respectively). Additionally, the relative fluorescent Ca^{2+} levels (ΔF) obtained from mitochondria are shown in black. The graph shows individual values with the media \pm SEM. The t tests performed on the Ca^{2+} indicators in each group as compared to a theoretical mean of no change ($\Delta F = 1$) revealed significant higher (** $p < 0.01$; * $p < 0.05$) and lower (### $p < 0.01$; # $p < 0.05$) Ca^{2+} levels after blue light stimulation (50 cells from 2–4 independent experiments).

present results reinforce the intrinsic light sensitivity of MC as shown by the Ca^{2+} increase specifically elicited by a BL pulse and totally absent after red light stimulation (Figure 1B and C). Moreover, we have previously reported that blue light has a significant effect on Opn3 levels and intracellular localization in primary MC cultures, through a mechanism of light induction dependent at least in part on *de novo* synthesis of protein (Rios et al., 2019). Interestingly, levels of Opn3 protein are tightly regulated by light stimulation in MC (Rios et al., 2019), neurons (unpublished data) and dermal fibroblasts (Lan et al., 2020).

Ca^{2+} signalling in glial cells represents an integral part of its physiology and, particularly in astrocytes, Ca^{2+} signals have been observed as spontaneous activity and G-coupled receptors-driven responses (McNeill et al., 2021). Ultimately the activation of these receptors leads to the production of inositol 1,4,5-trisphosphate (IP3) which binds to and activates IP3 receptors on the endoplasmic reticulum membrane, thereby releasing Ca^{2+} from intracellular stores (Holtzclaw et al., 2002; McNeill et al., 2021). Opsins are photopigments consisting of a G protein-coupled receptor (the apoprotein), and a retinaldehyde derived from vitamin A (the chromophore). Even though they are a monophyletic branch within the G protein-coupled receptor (GPCR) superfamily, the type of G protein to which the receptor is coupled varies, depending on the cell type, the tissue in which they are expressed or the species (Guido et al., 2020; Porter et al., 2011). Significant changes in somatic Ca^{2+} levels upon light stimulation have long been reported as intrinsic photic responses in diverse retinal cells such as visual photoreceptor cells, intrinsically photosensitive retinal ganglion cells and Opn4x-expressing horizontal cells (Contín et al., 2010; Díaz et al., 2017; Meister & Tessier-Lavigne, 2013; Morera et al., 2016; Nieto et al., 2011; Qiu et al., 2005), denoting a

typical characteristic of vertebrate photosensitivity. Our present results indicate that BL stimulation increases intracellular Ca^{2+} levels in MC by Ca^{2+} mobilization from internal stores (Figure 2A), as light-evoked responses were suppressed up to 50% after depletion of intracellular Ca^{2+} stores with TG (Figure 2C and 5), whereas no significant effects were observed when extracellular Ca^{2+} availability was modified by EGTA treatment (Figure 2B and 3). Indeed, we show a time correspondence between Ca^{2+} increase in the cytosol and Ca^{2+} decrease in the endoplasmic reticulum (Figure 5A), with significant overall Ca^{2+} changes along time for both compartments (Figure 6). Meanwhile, mitochondrial Ca^{2+} was not affected by BL stimulation (Figure 4D and E, Figure 6) suggesting that the light induction of Ca^{2+} increase in MC can be clearly restricted to a signaling cascade that mobilizes Ca^{2+} from endoplasmic reticulum.

Although most MC in the cultures expressed Opn3 (Figure 1 and Suppl. Figure 1), more than half of them exhibited significant light responses involving Ca^{2+} increase. The remaining non-responding cells could exhibit different active states for the opsin or different signaling cascades not necessarily involving calcium increase (i.e. cyclic nucleotides as described for heterologous expression of Opn3 chimeras by Sugihara et al., 2016). Moreover, these cells may need longer exposure times or brighter BL stimulation; since we applied the minimum stimulus required to identify calcium responses in MC, the presence of different MC populations could rely on stimulus characteristics including duration and intensity. Nevertheless, mixed populations of MC responding/non-responding to non-photic cues with calcium increase are in agreement with previous results by other authors (Newman, 2004; Rosa et al., 2015; Uckermann et al., 2002). Opn3 is phylogenetically included in vertebrate

visual opsins group and closely related to teleost multiple tissue opsin (TMT) which is expressed in teleosts and shows sensitivity to BL by activating the G_i protein cascade, thus decreasing cyclic adenosine monophosphate (cAMP) values (Kato et al., 2016). In line with this result the expression of chimeric proteins for Opn3 suggests that this opsin could directly modify cAMP concentration (Sugihara et al., 2016); however Opn3 stimulation in melanocytes and human fibroblasts implies the activation of PLC with a consequent increase in intracellular Ca^{2+} levels and downstream activation of CAMKII, JUNK, p38, ERK and CREB (Lan et al., 2020; Regazzetti et al., 2018). In the same direction, light-promoted regulation of cellular metabolism in brown adipocytes implies Opn3 activation and a GPCR mediated signaling pathway (Sato et al., 2020). Nevertheless, Ca^{2+} increase in glial cells has been related to G_i signaling as well, as for the registered responses after GABA stimulation in astrocytes (Durkee et al., 2019). So far, our previous (Rios et al., 2019) and present results strongly suggest that light-driven intrinsic Ca^{2+} responses in MC involves a BL sensitive opsin activation that signals for Ca^{2+} release from the endoplasmic reticulum, though more experiments should be carried out in order to properly identify the signaling cascade for the non-visual opsin mediating blue light responses in MC in cultures.

Initially described as passive cells in-between neurons, glial cells are presently considered a complex and dynamic cell type, which cannot generate an action potential, though they are able to respond biochemically to stimuli within their environment (McNeill et al., 2021). The development of advanced optical imaging techniques for the visualization of intracellular Ca^{2+} concentrations, revealed a complex system, underpinning this electrically non-excitabile cell type, where ion-mediated signals are highly regulated in space and time (Semyanov et al., 2020). Ca^{2+} increases in glial cells are observed as spontaneous transients, GPCR-mediated and glia-glia direct communication through gap junctions. When considering MC physiology, light is an environmental stimulus that has been previously addressed (Newman, 2003, 2005; Rillich et al., 2009) and described as a secondary response by MC to retinal ganglion cell light-stimulation. In this sense, repeated flash light stimulation to the rat retina increases Ca^{2+} transients frequency, with low and fast responses probably mediated by ganglion cells activation and ATP release (Newman, 2005). In the guinea pig retina MC cytosolic Ca^{2+} rises in response to repetitive light stimulation (over 10 min) consisting of two components: a slowly developing immediate response, evoked by neuron-to-glia signaling, and a delayed fast response evoked by a release of Ca^{2+} from intracellular stores (Rillich et al., 2009). Our results indicate a direct photo-activation of 70% of the analyzed MC, evidenced by a long-lasting increase cytosolic Ca^{2+} (up to 4 min after the stimulus, Figure 2A) as a result of Ca^{2+} release from the endoplasmic reticulum (Figure 5A), after BL stimulation for at least 20 s (no

responses were registered with shorter times of BL stimulation, unpublished data). These characteristics resemble some aspects of the described responses for melanopsin light activation in retinal neurons (Kumbalasisiri et al., 2007; Morera et al., 2016). Regarding glial cells, similar results have been previously described for the human MC line MIO-M1 that express a number of different opsins and respond with Ca^{2+} increases over several minutes to repetitive stimulation with 480 nm light (Hollborn et al., 2011). Blue light activation of viral transfected Opn4 in astrocytes elicits similar responses as they are observed in 75% of selected ROIs after at least 20 s of irradiance and lasting for several minutes (Mederos et al., 2019). These authors propose a new optogenetic approach to study Ca^{2+} dynamics in astrocytes resembling the physiological characteristics of Ca^{2+} mobilization by GPCR in this cell type. Understanding the intrinsic photosensitivity of MC might open a whole new chapter of light-driven responses in retinal physiology. Indeed, recent evidence indicates that MC modify the 11-cis-retinol pool via RGR-light detection and therefore, via their intrinsic photosensitivity, controlling cone's photosensitivity by regulating pigment regeneration independently of the already known metabolic pathways (Morshedian et al., 2019). In addition, considering that Ca^{2+} increase in mitochondria are related to oxidative stress events and apoptotic signaling (Agarwal et al., 2017; Carpio et al., 2021), our present results showing no changes in mitochondrial Ca^{2+} levels after BL stimulation (Figure 4C) further support a physiological role for MC intrinsic photo-detection. In fact, mitochondria-driven Ca^{2+} microdomains in astrocytes are elicited by light stimulation at 488 nm and mediated by reactive oxygen species production rather than constituting a photic response (Agarwal et al., 2017).

Overall, our findings shed light on a more complex level of light detection and intrinsic photosensitivity in different retinal cells including MC, showing them to be capable of greater involvement in the functioning of retinal circuits, cooperating with other photoreceptors to detect and integrate ambient light and participate in cell to cell communication.

Acknowledgments

Authors are grateful to Fabricio Navarro, Dr. Carlos Mas and Dr. Cecilia Sampedro for their excellent technical support at the CEMINCO facility and to Dr. Marcos Carpio for the kind gift of the Ca^{2+} indicator dyes Mag-Fluo-4/AM and Rhod-2/AM.

Author Contribution

N.A.M., M.N.R. and M.E.G. designed research; N.A.M. and M.N.R. performed research; M.E.G. contributed new reagents/analytic tools; N.A.M., M.N.R., and M.E.G. analyzed and discussed data; NAM and M.E.G. wrote the paper. M.N.R. revised the manuscript.


Declaration of Conflicting Interests

The authors declare that the research was conducted in the absence of any commercial or financial relationships that could be construed as a potential conflict of interest.

Funding

The author(s) disclosed receipt of the following financial support for the research, authorship, and/or publication of this article: This work was supported by the Fondo para la Investigación Científica y Tecnológica (grant number PICT 2017 Nr 0631, PICT 2016 Nr 0187, SECyT-UNC Consolidar 2018-2022).

ORCID iD

Mario E. Guido  <https://orcid.org/0000-0002-5485-4904>

Supplemental material

Supplemental material for this article is available online.

References

- Agarwal, A., Wu, P.-H., Hughes, E. G., Fukaya, M., Tischfield, M. A., Langseth, A. J., Wirtz, D., Bergles, D. E. (2017). Transient opening of the mitochondrial permeability transition pore induces microdomain calcium transients in astrocyte processes. *Neuron*, *93*(3), 587–605.e7. <https://doi.org/10.1016/j.neuron.2016.12.034>
- Barnett, N. L., Pow D, V. (2000). Antisense knockdown of GLAST, a glial glutamate transporter, compromises retinal function. *Investigative Ophthalmology & Visual Science*, *41*(2), 585–591. <https://iovs.arvojournals.org/article.aspx?articleid=2199863>
- Berson, D. M., Dunn, F. A., Takao, M. (2002). Phototransduction by retinal ganglion cells that set the circadian clock. *Science (New York, N.Y.)*, *295*(5557), 1070–1073. <https://doi.org/10.1126/science.1067262>
- Bringmann, A., Pannicke, T., Grosche, J., Francke, M., Wiedemann, P., Skatchkov, S. N., Osborne, N. N., Reichenbach, A. (2006). Müller cells in the healthy and diseased retina. *Progress in Retinal and Eye Research*, *25*(4), 397–424. <https://doi.org/10.1016/j.preteyeres.2006.05.003>
- Buhr, E. D., Yue, W. W. S., Ren, X., Jiang, Z., Liao, H. W. R., Mei, X., Vemaraju, S., Nguyen, M. T., Reed, R. R., Lang, R. A., Yau, K. W., Van Gelder, R. N. (2015). Neuropsin (OPN5)-mediated photoentrainment of local circadian oscillators in mammalian retina and cornea. *Proceedings of the National Academy of Sciences of the United States of America*, *112*(2), 13093–13098. <https://doi.org/10.1073/pnas.1516259112>
- Carpio, M. A., Katz, S. G. (2019). Methods to probe calcium regulation by BCL-2 family members. *Methods in Molecular Biology*, *1877*, 173–183. https://doi.org/10.1007/978-1-4939-8861-7_12
- Carpio, M. A., Means, R. E., Brill, A. L., Sainz, A., Ehrlich, B. E., Katz, S. G. (2021). BOK Controls apoptosis by Ca²⁺ transfer through ER-mitochondrial contact sites. *Cell Reports*, *34*(10), 108827. <https://doi.org/10.1016/j.celrep.2021.108827>
- Chaurasia, S., Rollag, M., Jiang, G., Hayes, W., Haque, R., Natesan, A., Zatz, M., Tosini, G., Liu, C., Korf, H., Iuvone, P., Provencio, I. (2005). Molecular cloning, localization and circadian expression of chicken melanopsin (Opn4): Differential regulation of expression in pineal and retinal cell types. *Journal of Neurochemistry*, *92*(1), 158–170. <https://doi.org/10.1111/j.1471-4159.2004.02874.x>
- Contin, M. A., Verra, D. M., Guido, M. E., Ana Contin, M., Verra, D. M., Guido, M. E. (2006). An invertebrate-like phototransduction cascade mediates light detection in the chicken retinal ganglion cells. *FASEB Journal*, *20*(14), 2648–2650. <https://doi.org/10.1096/fj.06-6133fje>
- Contín, M. A., Verra, D. M., Salvador, G., Ilincheta, M., Giusto, N. M., Guido, M. E. (2010). Light activation of the phosphoinositide cycle in intrinsically photosensitive chicken retinal ganglion cells. *Investigative Ophthalmology & Visual Science*, *51*(11), 5491–5498. <https://doi.org/10.1167/iovs.10-5643>
- Davies, W. L., Hankins, M. W., Foster, R. G. (2010). Vertebrate ancient opsin and melanopsin: Divergent irradiance detectors. *Photochem Photobiol Sci Off J Eur Photochem Assoc Eur Soc Photobiol*, *9*(11), 1444–1457. <https://doi.org/10.1039/c0pp00203h>
- Díaz, N. M., Morera, L. P., Tempesti, T., Guido, M. E. (2017). The visual cycle in the inner retina of chicken and the involvement of retinal G-protein-coupled receptor (RGR). *Molecular Neurobiology*, *54*(4), 2507–2517. <https://doi.org/10.1007/s12035-016-9830-5>
- Durkee, C. A., Covelo, A., Lines, J., Kofuji, P., Aguilar, J., Araque, A. (2019). G(i/o) protein-coupled receptors inhibit neurons but activate astrocytes and stimulate gliotransmission. *Glia*, *67*(6), 1076–1093. <https://doi.org/10.1002/glia.23589>
- Guido, M. E., Marchese, N. A., Rios, M. N., Morera, L. P., Diaz, N. M., Garbarino-Pico, E., Contin, M. A. (2020). Non-visual opsins and novel photo-detectors in the vertebrate inner retina mediate light responses within the blue spectrum region. *Cellular and Molecular Neurobiology*, *42*(1), 59–83. <https://doi.org/10.1007/s10571-020-00997-x>
- Hattar, S., Lucas, R., Mrosovsky, N., Thompson, S., Douglas, R., Hankins, M., Lem, J., Biel, M., Hofmann, F., Foster, R., Yau, K. (2003). Melanopsin and rod-cone photoreceptive systems account for all major accessory visual functions in mice. *Nature*, *424*(424), 76–81. <https://doi.org/10.1038/nature01761>
- Hollborn, M., Ulbricht, E., Rillich, K., Dukic-Stefanovic, S., Wurm, A., Wagner, L., Reichenbach, A., Wiedemann, P., Limb, G. A., Bringmann, A., Kohen, L. (2011). The human müller cell line MIO-M1 expresses opsins. *Molecular Vision*, *17*, 2738–2750. PMID: 22065927. PMCID: PMC3209432
- Holtzman, L. A., Pandhit, S., Bare, D. J., Mignery, G. A., Russell, J. T. (2002). Astrocytes in adult rat brain express type 2 inositol 1,4,5-trisphosphate receptors. *Glia*, *39*(1), 69–84. <https://doi.org/10.1002/glia.10085>
- Jorstad, N. L., Wilken, M. S., Todd, L., Finkbeiner, C., Nakamura, P., Radulovich, N., Hooper, M. J., Chitsazan, A., Wilkerson, B. A., Rieke, F., Reh, T. A. (2020). STAT Signaling modifies Ascl1 chromatin binding and limits neural regeneration from Muller glia in adult mouse retina. *Cell Reports*, *30*(7), 2195–2208.e5. <https://doi.org/10.1016/j.celrep.2020.01.075>
- Kato, M., Sugiyama, T., Sakai, K., Yamashita, T., Fujita, H., Sato, K., Tomonari, S., Shichida, Y., Ohuchi, H. (2016). Two opsin 3-related proteins in the chicken retina and brain: A TMT-type opsin 3 is a blue-light sensor in retinal horizontal cells, hypothalamus, and cerebellum. *PLoS One*, *11*(11), 1–23. <https://doi.org/10.1371/journal.pone.0163925>

- Kumbalasisri, T., Rollag, M. D., Isoldi, M. C., Castrucci, A. d. L., Provencio, I. (2007). Melanopsin triggers the release of internal calcium stores in response to light. *Photochemistry and Photobiology*, 83(2), 273–279. <https://doi.org/10.1562/2006-07-11-RA-964>
- Lan, Y., Wang, Y., Lu, H. (2020). Opsin 3 is a key regulator of ultraviolet A-induced photoageing in human dermal fibroblast cells. *British Journal of Dermatology*, 182(5), 1228–1244. <https://doi.org/10.1111/bjd.18410>
- Lucas, R. J., Hattar, S., Takao, M., Berson, D. M., Foster, R. G., Yau, K.-W. (2003). Diminished pupillary light reflex at high irradiances in melanopsin-knockout mice. *Science (New York, N.Y.)*, 299(5604), 245–247. <https://doi.org/10.1126/science.1077293>
- Mansoor, S., Sharma, A., Cáceres-del-Carpio, J., Zacharias, L. C., Patil, A. J., Gupta, N., Limb, G. A., Kenney, M. C., Kuppermann, B. D. (2015). Effects of light on retinal pigment epithelial cells, neurosensory retinal cells and müller cells treated with brilliant blue G. *Clinical & Experimental Ophthalmology*, 43(9), 820–829. <https://doi.org/10.1111/ceo.12568>
- McNeill, J., Rudyk, C., Hildebrand, M. E., Salmaso, N. (2021). Ion channels and electrophysiological properties of astrocytes: implications for emergent stimulation technologies. *Frontiers in Cellular Neuroscience*, 15, 1–22. <https://doi.org/10.3389/fncel.2021.644126>
- Mederos, S., Hernández-Vivanco, A., Ramírez-Franco, J., Martín-Fernández, M., Navarete, M., Yang, A., Boyden, E. S., Perea, G. (2019). Melanopsin for precise optogenetic activation of astrocyte-neuron networks. *Glia*, 67(5), 915–934. <https://doi.org/10.1002/glia.23580>
- Meister, M., Tessier-Lavigne, M. (2013). Low-level visual processing: The retina. *Princ neural Sci*, 5, 577–601.
- Morera, L. P., Díaz, N. M., Guido, M. E. (2012). A novel method to prepare highly enriched primary cultures of chicken retinal horizontal cells. *Experimental Eye Research*, 101, 44–48. <https://doi.org/10.1016/j.exer.2012.05.010>
- Morera, L. P., Díaz, N. M., Guido, M. E. (2016). Horizontal cells expressing melanopsin x are novel photoreceptors in the avian inner retina. *Proceedings of the National Academy of Sciences of the United States of America*, 113(46), 13215–13220. <https://doi.org/10.1073/pnas.1608901113>
- Morshedian, A., Kaylor, J. J., Ng, S. Y., Tsan, A., Frederiksen, R., Xu, T., Yuan, L., Sampath, A. P., Radu, R. A., Fain, G. L., Travis, G. H. (2019). Light-Driven regeneration of cone visual pigments through a mechanism involving RGR opsin in müller glial cells. *Neuron*, 102(6), 1172–1183.e5. <https://doi.org/10.1016/j.neuron.2019.04.004>
- Newman, E. A. (2003). Glial cell inhibition of neurons by release of ATP. *Journal of Neuroscience*, 23(5), 1659–1666. <https://doi.org/10.1523/JNEUROSCI.23-05-01659.2003>
- Newman, E. A. (2004). Glial modulation of synaptic transmission in the retina. *Glia*, 47(3), 268–274. <https://doi.org/10.1002/glia.20030>
- Newman, E. A. (2005). Calcium increases in retinal glial cells evoked by light-induced neuronal activity. *Journal of Neuroscience*, 25(23), 5502–5510. <https://doi.org/10.1523/JNEUROSCI.1354-05.2005>
- Newman, E. A. (2015). Glial cell regulation of neuronal activity and blood flow in the retina by release of gliotransmitters. *Philos trans R Soc London Ser B. Biol Sci*, 370(1672). <https://doi.org/10.1098/rstb.2014.0195>
- Nieto, P. S., Valdez, D. J., Acosta-Rodríguez, V. A., Guido, M. E. (2011). Expression of novel opsins and intrinsic light responses in the mammalian retinal ganglion cell line RGC-5. Presence of Opn5 in the rat retina. *PLoS One*, 6(10). <https://doi.org/10.1371/journal.pone.0026417>
- Pannicke, T., Ivo Chao, T., Reisenhofer, M., Francke, M., Reichenbach, A. (2017). Comparative electrophysiology of retinal müller glial cells—A survey on vertebrate species. *Glia*, 65(4), 533–568. <https://doi.org/10.1002/glia.23082>
- Pannicke, T., Uckermann, O., Iandiev, I., Wiedemann, P., Reichenbach, A., Bringmann, A. (2005). Ocular inflammation alters swelling and membrane characteristics of rat müller glial cells. *Journal of Neuroimmunology*, 161(1-2), 145–154. <https://doi.org/10.1016/j.jneuroim.2005.01.003>
- Peirson, S. N., Haiford, S., Foster, R. G. (2009). The evolution of irradiance detection: melanopsin and the non-visual opsins. *Philos Trans R Soc B Biol Sci*, 364(1531), 2849–2865. <https://doi.org/10.1098/rstb.2009.0050>
- Pfeiffer-Guglielmi, B., Francke, M., Reichenbach, A., Fleckenstein, B., Jung, G., Hamprecht, B. (2005). Glycogen phosphorylase isozyme pattern in mammalian retinal müller (glial) cells and in astrocytes of retina and optic nerve. *Glia*, 49(1), 84–95. <https://doi.org/10.1002/glia.20102>
- Porter, M. L., Blasic, J. R., Bok, M. J., Cameron, E. G., Pringle, T., Cronin, T. W., Robinson, P. R. (2011). Shedding new light on opsin evolution. *Proc R Soc B Biol Sci*, 279(1726), 3–14. <https://doi.org/10.1098/rspb.2011.1819>
- Qiu, X., Kumbalasisri, T., Carlson, S. M., Wong, K. Y., Krishna, V., Provencio, I., Berson, D. M. (2005). Induction of photosensitivity by heterologous expression of melanopsin. *Nature*, 433(7027), 745–749. <https://doi.org/10.1038/nature03345>
- Regazzetti, C., Sormani, L., Debayle, D., Bernerd, F., Tulic, M. K., De Donatis, G. M., Chignon-Sicard, B., Rocchi, S., Passeron, T. (2018). Melanocytes sense blue light and regulate pigmentation through opsin-3. *Journal of Investigative Dermatology*, 138(1), 171–178. <https://doi.org/10.1016/j.jid.2017.07.833>
- Rillich, K., Gentsch, J., Reichenbach, A., Bringmann, A., Weick, M. (2009). Light stimulation evokes two different calcium responses in müller glial cells of the Guinea pig retina. *European Journal of Neuroscience*, 29(6), 1165–1176. <https://doi.org/10.1111/j.1460-9568.2009.06682.x>
- Rios, M. N., Marchese, N. A., Guido, M. E. (2019). Expression of Non-visual opsins Opn3 and Opn5 in the developing inner retinal cells of birds. Light-responses in müller glial cells. *Frontiers in Cellular Neuroscience*, 13, 1–14. <https://doi.org/10.3389/fncel.2019.00376>
- Rosa, J. M., Bos, R., Sack, G. S., Fortuny, C., Agarwal, A., Bergles, D. E., Flannery, J. G., Feller, M. B. (2015). Neuron-glia signaling in developing retina mediated by neurotransmitter spillover. *Elife*, 4, 1–20. <https://doi.org/10.7554/eLife.09590>
- Sato, M., Tsuji, T., Yang, K., Ren, X., Dreyfuss, J. M., Huang, T. L., Wang, C. H., Shamsi, F., Leiria, L. O., Lynes, M. D., Yau, K. W., Tseng, Y. H. (2020). Cell-autonomous light sensitivity via Opsin3 regulates fuel utilization in brown adipocytes. *PLoS Biology*, 18(2), 1–27. <https://doi.org/10.1371/journal.pbio.3000630>
- Semyanov, A., Henneberger, C., Agarwal, A. (2020). Making sense of astrocytic calcium signals — from acquisition to interpretation. *Nature Reviews Neuroscience*, 21(10), 551–564. <https://doi.org/10.1038/s41583-020-0361-8>

- Sugihara, T., Nagata, T., Mason, B., Koyanagi, M., Terakita, A. (2016). Absorption characteristics of vertebrate non-visual opsin, *Opn3*. *PLoS One*, *11*(8), 1–15. <https://doi.org/10.1371/journal.pone.0161215>
- Uckermann, O., Grosche, J., Reichenbach, A., Bringmann, A. (2002). ATP-evoked calcium responses of radial glial (müller) cells in the postnatal rabbit retina. *Journal of Neuroscience Research*, *70*(2), 209–218. <https://doi.org/10.1002/jnr.10406>
- Valdez, D. J., Nieto, P. S., Díaz, N. M., Garbarino-Pico, E., Guido, M. E. (2013). Differential regulation of feeding rhythms through a multiple-photoreceptor system in an avian model of blindness. *FASEB J Off Publ Fed Am Soc Exp Biol*, *27*(7), 2702–2712. <https://doi.org/10.1096/fj.12-222885>
- Valdez, D. J., Nieto, P. S., Garbarino-Pico, E., Avalle, L. B., Díaz-Fajreldines, H., Schurrer, C., Cheng, K. M., Guido, M. E. (2009). A nonmammalian vertebrate model of blindness reveals functional photoreceptors in the inner retina. *FASEB Journal*, *23*(4), 1186–1195. <https://doi.org/10.1096/fj.08-117085>
- Wagner, P. M., Sosa Alderete, L. G., Gorné, L. D., Gaveglio, V., Salvador, G., Pasquaré, S., Guido, M. E. (2019). Proliferative Glioblastoma Cancer Cells Exhibit Persisting Temporal Control of Metabolism and Display Differential Temporal Drug Susceptibility in Chemotherapy. *Mol Neurobiol*, *56*(2), 1276–1292. <https://doi.org/10.1007/s12035-018-1152-3>
- Willbold, E., Rothermel, A., Tomlinson, S., Layer, P. G. (2000). Müller glia cells reorganize reaggregating chicken retinal cells into correctly laminated in vitro retinæ. *Glia*, *29*(1), 45–57. [https://doi.org/10.1002/\(SICI\)1098-1136\(20000101\)29:1<45::AID-GLIA5>3.0.CO;2-4](https://doi.org/10.1002/(SICI)1098-1136(20000101)29:1<45::AID-GLIA5>3.0.CO;2-4)
- Abbreviations**
- | | | | |
|--------|---|--------|--|
| EGTA | 3,12-Bis(carboxymethyl)-6,9-dioxa-3,12-diazatetradecane-1,14-dioic acid | GPCR | G protein-coupled receptor |
| DAPI | 40,6-diamidino-2-phenylindole | GABA | gamma-Aminobutyric acid |
| BL | Blue Light | GFAP | Glial fibrillary acidic protein |
| CMF | Ca ⁺² -Mg ⁺² free Tyrode's buffer | GLAST1 | Glutamate-aspartate Transporter |
| CAMKII | Ca ²⁺ /calmodulin-dependent protein kinase II | GS | Glutamine synthetase |
| CREB | cAMP response element-binding protein | IP3 | Inositol 1,4,5-trisphosphate |
| JUNK | c-jun N-terminal kinase | MC | Müller glial cells |
| cAMP | Cyclic adenosine monophosphate | NIF | Non image forming |
| DMEM | Dulbecco's modified Eagle's medium | p38 | p38 mitogen-activated protein kinase |
| E8 | Embryonic Day 8 | PBS | Phosphate-buffered saline |
| ERK | Extracellular signal-regulated kinases" | PLC | Phospholipase C |
| FBS | Fetal Bovine Serum | RGR | Retinal G protein-coupled receptor |
| | | TMT | Teleost multiple tissue opsin |
| | | TG | Thapsigargin |
| | | AD | no expansion possible |
| | | ARS | sodium arsenite |
| | | ARVO | Association for Research in Vision and Ophthalmology |
| | | ATP | adenosine triphosphate, BD: no expansion possible |
| | | BSA | Bovine serum albumin |
| | | COR | no expansion possible |
| | | DMSO | Dimethyl sulfoxide |
| | | GLAST | Glutamate Aspartate Transporter |
| | | LED | light emitting diode |
| | | MCO | no expansion possible |
| | | MIO-M1 | Moorfields Institute of Ophthalmology-Müller 1 |
| | | M-MLV | Moloney Murine Leukemia Virus |
| | | MTT | 3-(4,5-dimethylthiazol-2-yl)-2,5-diphenyltetrazolium bromide |
| | | NA | no expansion possible |
| | | PCR | polymerase chain reaction |
| | | RIPA | no expansion possible |
| | | ROI | Region of interest |
| | | RT | room temperature |
| | | SANYO | no expansion possible |
| | | SDS | Sodium Dodecyl Sulfate |
| | | SEM | Standard error of the media |
| | | SERCA | sarco/endoplasmic reticulum Ca ²⁺ -ATPase |
| | | SRL | no expansion possible |
| | | UV | Ultraviolet. |